

Analysis of Complex Flow Patterns with Acceleration-Encoded MRI

F. Staehle¹, S. Bauer¹, B. Jung¹, J. Hennig¹, and M. Markl¹

¹Department of Diagnostic Radiology, University Hospital Freiburg, Freiburg, Germany

Introduction: The phase contrast principle (PC) can be employed to measure flow acceleration by using acceleration sensitive encoding gradients. The direct assessment of regional acceleration can provide valuable information regarding changes in timing (temporal acceleration) and direction (convective acceleration) of flow. Although acceleration data may be estimated from velocity encoded images, the direct measurement of acceleration may be advantageous due to amplification of velocity noise by error propagation when calculating spatio-temporal velocity derivatives [1-3]. The aim of this study was to evaluate a newly developed gradient optimized acceleration-sensitive MRI technique with full three-directional acceleration encoding of aortic blood flow. Results were compared to standard velocity encoded phase contrast MRI. In addition, the value of acceleration induced intravoxel dephasing as a new image contrast providing information about complex and vortical flow was investigated.

Methods: Five volunteer measurements (the left ventricular out-flow tract) were performed at 1.5T (n=2, Avanto, Siemens) and at 3T (n=3, Trio, Siemens). Three acceleration-encoded PC MRI sequences were implemented with sensitivities of $\pm 50 \text{ m/s}^2$, $\pm 100 \text{ m/s}^2$ and $\pm 150 \text{ m/s}^2$ in all three spatial directions. Gradient optimization and sequential acceleration encoding [4] resulted in comparatively short TE/TRs of 7.0-7.3/9.5-10ms, 5.9-6.2/8.3-8.8ms and 5.4-5.7/7.8-8.2ms and temporal resolutions of 19-20 ms, 16.6-17.6 ms and 15.6-16.4 ms. Velocity PC-MRI data were acquired with TE=2.6-2.8 ms and temporal resolutions of 19.2-20.8 and 37.2-39.2ms. Common parameters for all measurements were: matrix 256*169, FOV=360mm*360mm*8mm, BW=450Hz/Px, flipangle=15°. Data was corrected for Maxwell-terms and eddy-currents. Two ROIs, directly below the aortic valve and between the sinuses were used to calculate mean acceleration-time curves which were averaged over the five volunteers (Fig. 3). In the same ROIs, acceleration was approximated by the temporal derivative of the velocity data. Intravoxel dephasing associated with the vortex flow behind the right valve cusp (Fig. 2, top) and valve closure (Fig. 2, bottom) was quantified by their temporal persistence and spatial extent.

Results: Fig. 1 shows the fusion of the systolic velocity encoded data (vectors) with the acceleration encoded magnitude image in the left ventricular out-flow tract. Intravoxel dephasing in the sinuses clearly corresponded to the location of the flow vortices (white arrows). A direct comparison of magnitude images from acceleration and velocity encoding (Fig. 2) further demonstrates the sensitivity to detect vortical flow or valve closure which is not possible for velocity-sensitive MRI. Moreover, the overlay of acceleration data as contour plots (left) provides further information on regions with enhanced acceleration (black arrows) Fig. 3 and table 1 shows the acceleration data averaged over five volunteers for a sensitivity of 50 m/s^2 and the time derivative calculated from the velocity data. The deviation of the acceleration curve below the valve can be explained by the additional contribution of convective acceleration. On top of the curves, the extend and timing of the regions affected by intravoxel dephasing due to the valve vortices and the valve closing are shown. Intravoxel dephasing was mostly absent in the velocity images. The dephasing was reduced at lower acceleration sensitivities with a reduced duration for the left valve vortex from $227 \pm 18 \text{ ms}$ (50 m/s^2) to $184 \pm 26 \text{ ms}$ (100 m/s^2) and $176 \pm 19 \text{ ms}$. The maximum width was reduced from 5.4 mm (50 m/s^2) to 3.5 mm (100 m/s^2) and 3.7 mm (150 m/s^2).

	Proximal to valve Velocity Derivative	Distal to valve Velocity Derivative	Proximal to valve Measured Acceleration	Distal to valve Measured Acceleration
acc Max [m/s ²]	12,8 ± 2,2	17,6 ± 5,5	28,7 ± 4,9	15,2 ± 8,5
acc Min [m/s ²]	-9,8 ± 2,1	-9 ± 2	-12,4 ± 3,3	-9,3 ± 2
TTP Max [ms]	85 ± 11	98 ± 17	114 ± 26	82 ± 18
TTP Min [ms]	343 ± 21	360 ± 27	342 ± 11	314 ± 70

Table 1: Peak and time-to-peak (TTP)- acceleration, SD: variation 5 volunteers.

Discussion: Flow acceleration mapping with multi-directional encoding may provide an improved sensitivity for the detection of complex flow patterns such as vortex formation or swirling motion which include strong acceleration components. The nature of vortex flow or valve closure result in high sub-voxel convective acceleration which lead to intravoxel dephasing in the acceleration encoded images and thus signal loss thereby generating information about flow structure quicker than the postprocessing of phase images. Further work should focus on the applicability of the intravoxel dephasing image contrast to cardiovascular pathologies that could profit from quick diagnosis. Combination of velocity and acceleration encoded data may provide new insight into flow characteristics and their impact on local acceleration and intravoxel dephasing.

References: [1] Balleux-Buyens et al. Phys. Med. Biol. 51:4747-4758 [2] Tasu et al. MRM. 38:110-116 [3] Tasu et al. MRM. 44:66-72 [4] Staehle F et al, Proceedings of the ISMRM 2009 **Acknowledgements:** Deutsche Forschungsgemeinschaft (DFG), Grant # MA 2383/4-1; Bundesministerium für Bildung und Forschung (BMBF), Grant # 01EV0706

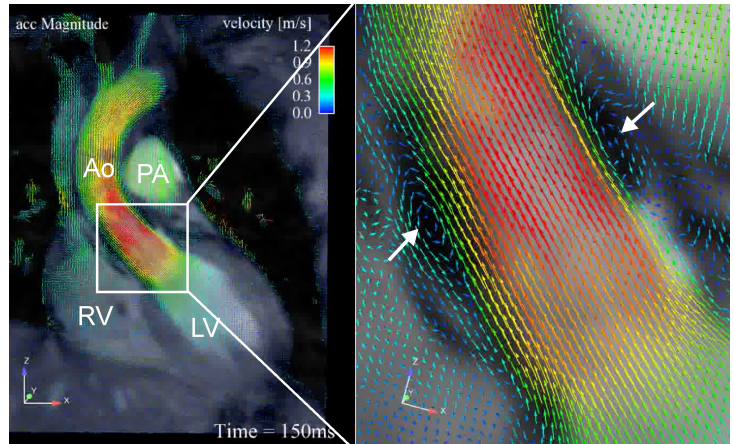


Figure 1: Left: Magnitude image of left ventricle and ascending aorta of a systolic phase. The vectors represent velocities measured with velocity encoding. Right: Enlarged view of sinuses with intravoxel dephasing in valve vortices (Arrows).

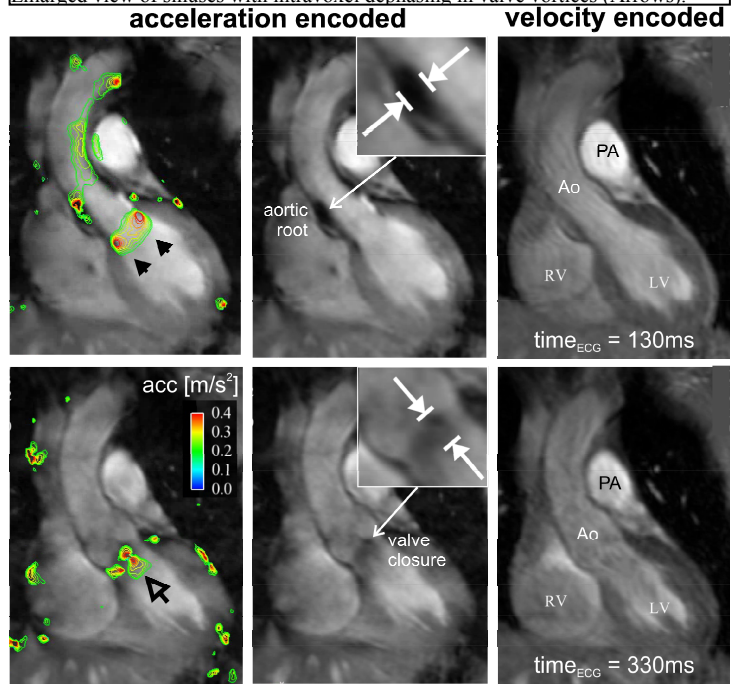


Figure 2: Contour plots (left) of the acceleration magnitude obtained by combining the acceleration information in the three spatial directions, magnitude images of acceleration encoding (center) and velocity encoding (right) during systole (top) and the valve closure (bottom).

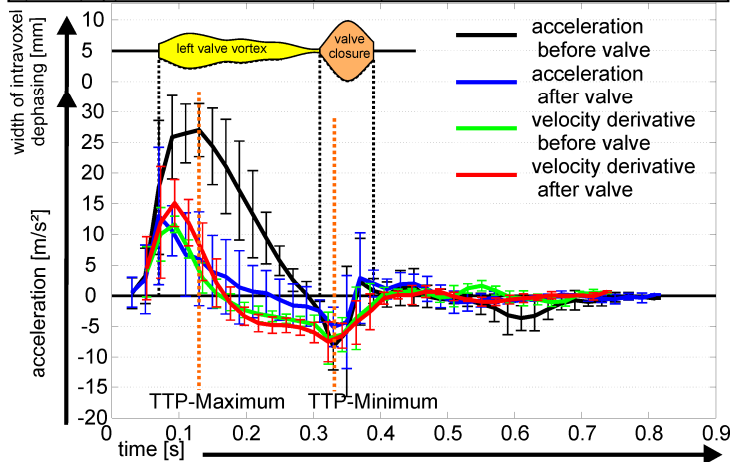


Figure 3: Time courses of measured acceleration and velocity derivatives along the ascending aorta averaged over five volunteers. Top: Width of intravoxel dephasing during systole (left valve vortex) and the valve closure.